JMEPEG (2021) 30:1906–1913
https://doi.org/10.1007/s11665-021-05541-6

Synthesis and Characterization of a Ni_3Al Intermetallic Modified with Copper Atoms via Powder Metallurgy

S.A. Serna, J.A. Verduzco, B.F. Campillo, A. Molina, R. Guardian, A. del Pozo, A. Sedano, and H. Villanueva

Submitted: 27 May 2020 / Revised: 27 December 2020 / Accepted: 28 January 2021 / Published online: 17 February 2021

Recent developments in the field of intermetallics have led to a renewed interest in system strengthening in order to improve their mechanical properties. In this work, the synthesis of $(Ni,Cu)_3Al$ at.% powders via the mechanical alloying technique is explored under different conditions. The study of NiAlCu alloys was carried out to determine the influence of copper additions on the microstructure and mechanical properties of a Ni_3Al intermetallic solid solution with copper substitutional atoms. The obtained compound was characterized by x-ray diffraction and scanning electron microscopy. The results show that during the mechanical alloying process a new intermetallic phase is formed with a higher energy regime of short duration, while at lower energy regimes, the increase in milling time only resulted in higher particle refinement. Therefore, it is shown that during the processing of the NiAlCu powders, the selection of the milling parameters plays a critical and sensitive role in the successful synthesis of $(Ni,Cu)_3Al$ powders via mechanical alloying.

Keywords intermetallic compounds, mechanical alloying, (Ni,Cu)3Al, powder metallurgy, x-ray diffraction

1. Introduction

Intermetallic compounds such as Ni_3Al are phases with more than two metal elements with an ordered structure and defined stoichiometry, these conditions provide intermetallic materials with properties such as high strength at elevated temperatures, low density, good thermal conductivity and good corrosion resistance (Ref 1–5). However, most of the Al-Ni system intermetallic synthesis has been made by conventional melting processes that although capable of improving the properties of the intermetallic material, the great temperature difference between aluminum and nickel causes segregation and nonhomogeneity in the intermetallic due to the rapid reaction of the nickel aluminides. In addition to this, intermetallic materials at room temperature can be very fragile (Ref 6), therefore the addition of elements such as Cu, B and Ni to improve the ductility of the intermetallic and changing their mechanical properties is important (Ref 6–8). Elements such as Te, Mo, W, Cr, Re, Ru, Co, and Ir have been studied which strengthen the mechanical properties of the Ni_3Al intermetallic (Ref 9–11). The intermetallic Ni_3Al has some excellent physical and chemical properties to be employed as a structural material, but its elastic limit at temperature range of 600-800°C tends to show anomalous behavior by drastically decreasing (Ref 12, 13). To counteract this effect, the intermetallic structure is modified with the addition of Cu. This article studies the effect of the milling speed and the addition of 25% Cu in the Ni_3Al intermetallic during the synthesis process by mechanical alloying (Ref 14, 15).

S.A. Serna, A. Molina, R. Guardian, A.del Pozo, and **A. Sedano**, Centro de Investigación en Ingeniería y Ciencias Aplicadas (UAEM) Cuernavaca Morelos, 62209 Cuernavaca, Mexico; **J.A. Verduzco** and **H. Villanueva**, Universidad Michoacana de San Nicolás de Hidalgo. (UMSNH) Morelia Michoacán, 58000 Morelia, Mexico; and **B.F. Campillo**, Instituto de Ciencias Físicas (UNAM) Cuernavaca Morelos, 62209 Cuernavaca, Mexico. Contact e-mail: heriberto.villanuevap@uaem.edu.mx.

2. Materials and Methods

2.1 Materials

High purity (> 99%) elemental Al, Ni, and Cu powders were used for the initial powder mixture. The morphology of the Al powders was flake-powder like with an average particle size of 18 μm and a thickness of 1 μm meanwhile, the morphology of the Cu powders was dendritic with a particle size of 2 μm, and the morphology of the Ni powders was amorphous with a particle size of 20 μm, Fig. 1. The composition of the synthesized nickel intermetallic samples corresponds to that of 50% nickel 25% copper, and 25% aluminum; the composition in wt.% values and properties of the initial powders are shown in Table 1.

2.2 Composite Processing

The synthesis of the Cu modified Ni_3Al powders was carried out in stainless steel vials with a 10:1 powder-ball ratio, in a low-energy planetary ball mill (FRITSCH Pulverisette) under an inert argon atmosphere with 3 ml of stearic acid as process control agent (PCA). This was done in order to reduce the risk of oxidation of the powders during the mechanical alloying process. Samples of the milled powders were obtained at speeds of 400, 450 and 500 rpm after a regime of 4, 8, 12, 16, 20, 24 and 30 h of milling time.

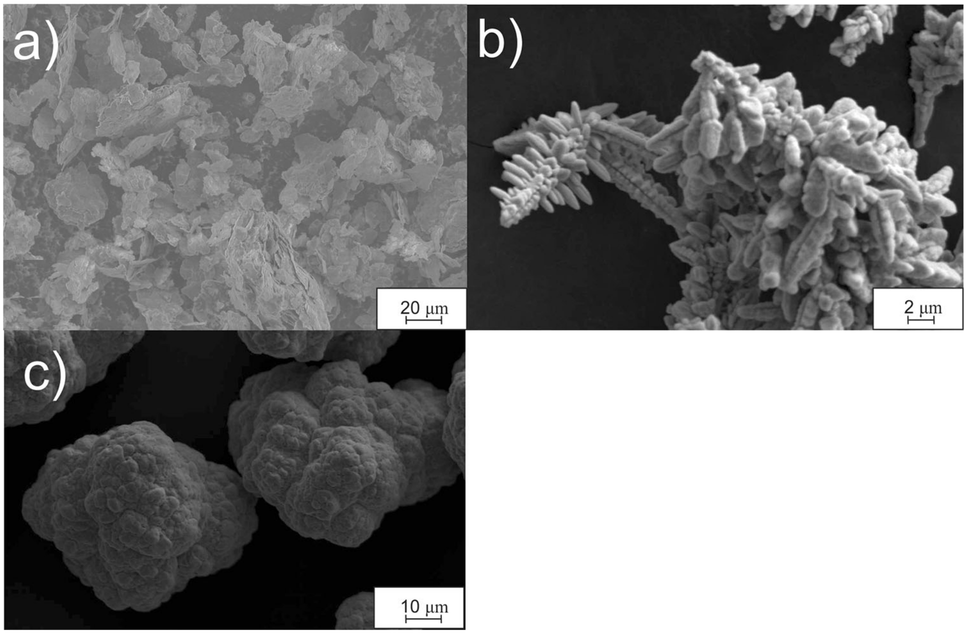

Fig. 1 Metallic elements used to fabricate the intermetallics, (a) aluminum flakes, (b) and (c) copper and nickel powders, respectively

Table 1 Raw material, composition and properties

Raw material	Atomic percent (at.%)	weight percent (wt.%)	Purity (%)	Average particle size (μm)
Nickel	50	2.25	99.995	20
Aluminum	25	0.5192	99.8	18
Copper	25	1.222	99.9	3

2.3 Materials Characterization

The obtained products were characterized by scanning electron microscopy (SEM) in a Leo 1450 vp Scanning Electron Microscope as well as by x-ray diffraction analysis obtained in a BRUKER D2 PHASER diffractometer with a copper radiation Kα a 40 kV and 25 mA in a range of 20–80°.

3. Results and Discussion

This paper investigates the influence of Cu addition on the structure of Ni_3Al intermetallic, synthesized by mechanical alloying. The final Ni-Al-Cu intermetallic samples obtained by the mechanical alloying technique from a mixture of powders with concentrations of 50–25–25 at.%, respectively, must correspond stoichiometrically with this composition after the powders become completely homogenized once the milling process finishes. The constant collisions with the balls during the mechanical alloying process are the main driving force behind the atomic diffusion of the powders during the mechanical alloying process, contrary to traditional methods this occurs at near room temperatures with the recurring events of cold-welding and fracture of the milled powders. Due to the above, the phase composition of the final powders is expected to correspond to that shown in the ternary phase diagram of Ni-Al-Cu (Fig. 2), in which the presence of the Ni_3Al intermetallic phase is observed with the addition of substitutional Cu atoms.

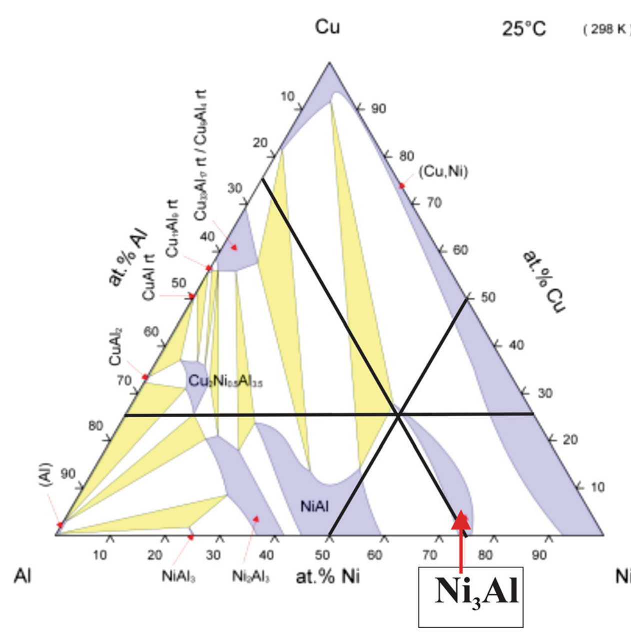

Fig. 2 Phase diagram at 25°C of Ni-Al-Cu system (22)

Sintered microporous intermetallics have gained attention due to their unique properties which promises a large range of potential applications, this requires that the sintered powders are composed of fine particles of the final intermetallic, so that during the densification phase of the powders, the size of the porosities reaches the micron scale. Continuous milling of the powders after reaching balance of the cold-welding and fracture events promotes the homogenization of powders as well as their refinement. Therefore, long time milling of intermetallic powders is encouraged for future applications (Ref 16).

3.1 X-ray Diffraction

The present study was designed to determine the effect of the milling speed on the initial powders, therefore the results of the x-ray analysis of the samples obtained at different milling revolutions are presented below, where different phenomena can be observed during the mechanical alloying process. The x-ray diffraction patterns of the samples obtained at 400 rpm are observed in Fig. 3, it is important to notice the presence of the elemental Ni, Al, and Cu peaks without the formation of secondary phases or oxides, furthermore, it is observed a decrease in intensity of the main nickel and copper peaks after 32 h of milling, this is mostly due to the phase forming stage during the mechanical alloying process(Ref 17), however, the peaks do not disappear completely, which indicates that the system needs more energy (higher revolutions) in order to achieve the phase change. The constant decrease of the particle size during the mechanical alloying process of the Ni, Cu, and Al powders exhibits a process with low energy, and therefore, a process with a reduced number of cold welding events with a high rate of particle fracture (Ref 18, 19). On the other hand, in Fig. 4 the x-ray diffraction patterns corresponding to the samples obtained at 450 rpm are shown. In this case, it is observed that by increasing the energy of the system during the mechanical alloying process (which results in a greater number of collisions events between balls per minute) the decrease in the intensity of XRD peaks is associated with peak broadening and peak shift toward lower angles therefor a phase change in the material is achieved after 24 h (Ref 20), with the formation of new peaks where the aluminum is diffusing in the structure of the Ni as well as the Cu atoms are replacing the corresponding Ni atoms with those of the intermetallic $(Ni,Cu)_3Al$ (Ref 2, 21). In addition to the above, greater refinement of the powders than that of the samples at 400 rpm is exhibited, since higher revolutions increase the fracture rate of the intermetallic particles, the main peak is found in the diffraction angle of 44.11° followed in intensity by those found in 51.24° and 75.29° respectively. Finally, the x-ray diffraction patterns of the samples at 500 rpm are presented in Fig. 5, in which it is observed that the time necessary for the formation of the intermetallic $(Ni,Cu)_3Al$ decreased due to the increase in energy in the system by the increase in revolutions. At this speed only 8 h are needed for the peaks of the initial powders to disappear and the phase change to occur. In the same way, it is observed that for these samples, the crystallite size was not reduced as in the samples at 400 and 450 rpm, therefore it can be concluded that at revolutions below 450rpm, the phenomenon that predominates is the fracture of Ni-Al-Cu particles while at higher revolutions the predominant events are cold welding and atomic diffusion, this is observed in the disappearance of the

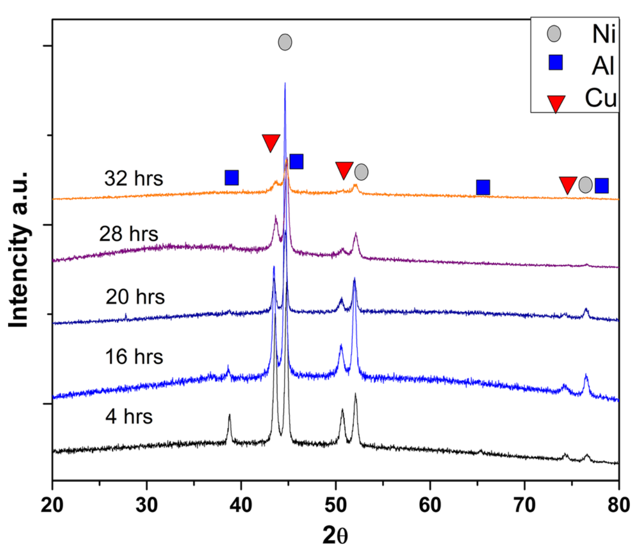

Fig. 3 X-ray diffraction patterns for the Ni-Al-Cu system mechanically alloyed at 400 rpm

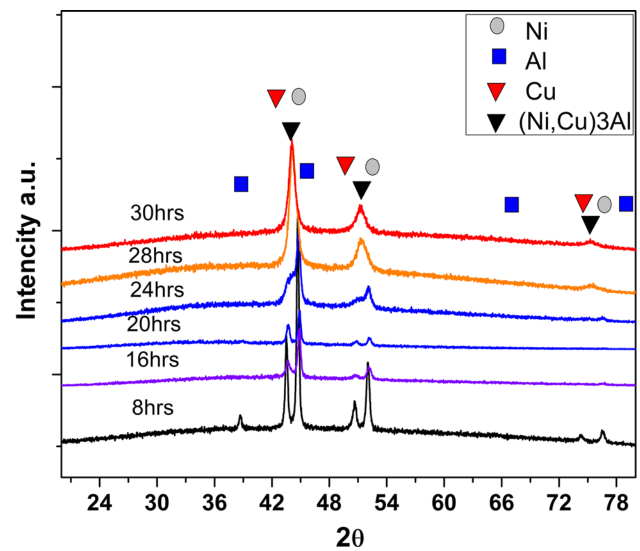

Fig. 4 X-ray diffraction patterns for the Ni-Al-Cu system mechanically alloyed at 450 rpm

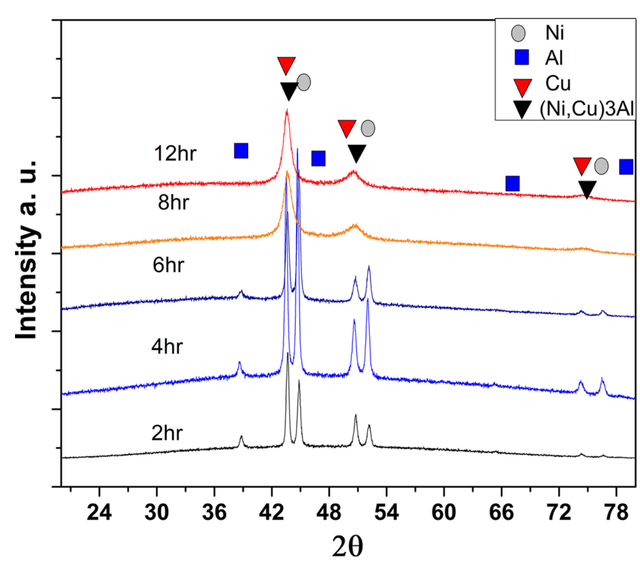

Fig. 5 X-ray diffraction patterns for the Ni-Al-Cu system mechanically alloyed at 500 rpm

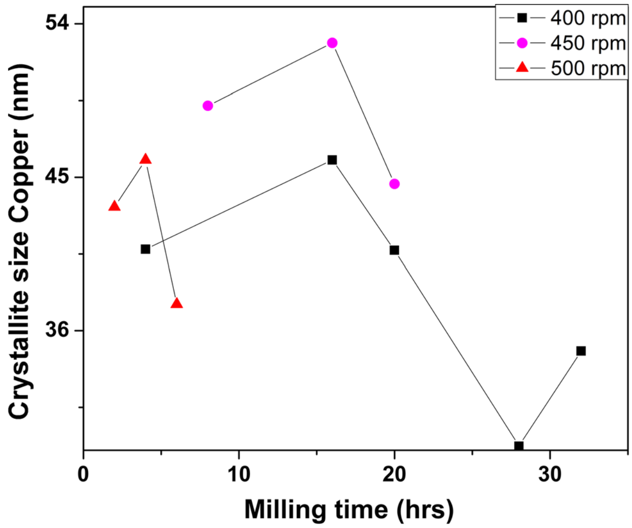

Fig. 6 Crystallite size of Copper as a function of the milling time

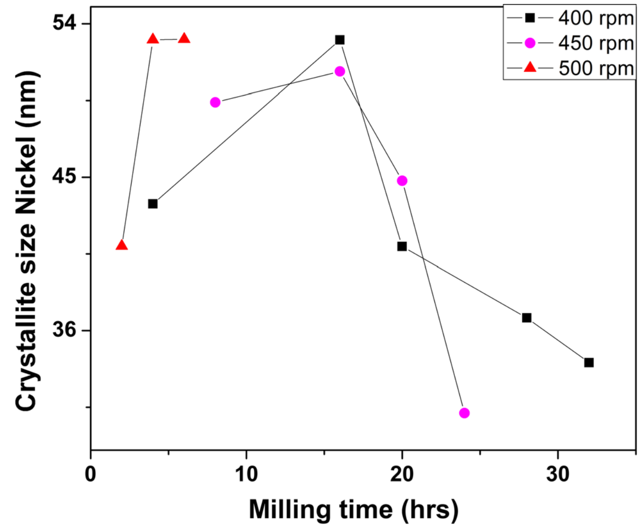

Fig. 7 Crystallite size of Nickel as a function of the milling time

main peaks of the initial powders and the presence of the main peaks of the $(Ni,Cu)_3Al$ intermetallic.

The widening of the diffraction peaks can be considered as a product of the refinement of the crystallite size powders as the grinding process proceeds. Figures 6 and 7, with small oscillations likely linked to the heating of powders occurring during the milling process, as well as an enhancement in potential energy by an increment in surface area of the powders and accumulation of defects, resulting in the reordering of the crystal structure and relaxation of the lattice. As the milling speed increases, the energy of the system does too, therefore the smallest crystallite sizes where observed on the sample which favored refinement over phase transformation, this will depend on the balance with cold-welding and fracture, therefore the Ni phase presented higher refinement at 400 rpm meanwhile the Cu phase at 450 rpm, attaining crystallite sizes of 27 nm and 35 nm, respectively (Ref 13).

For comparing purposes, XRD patterns of the Ni_3Al intermetallic synthetized at 500 rpm are shown in Fig. 8. These patterns exhibit only the presence of Ni and Al peaks as well as a higher rate of change during milling time compared to those modified with copper. This, in turn, results in a reduction of the milling time required to successfully synthesize the material, going from 12 h for the $(Ni,Cu)_3Al$ sample to 8h for the Ni_3Al sample. This behavior is related to a change in the cold welding/facture ratio, due to the high ductility of the copper powders, which reduces the fracture rate of the milled powders.

3.2 Scanning Electron Microscope (SEM)

The characterization by scanning electron microscopy is important to have a better understanding of the effect that the mechanical alloying technique exerts on the milled powders, as well as to determine the predominant phenomena during the process for the successful synthesis of the material. As previously described when milling at 400 revolutions, the intermetallic cannot be formed; in Fig. 9 it is seen that the powder is highly refined after 32 h, but there is not a noticeable change in the contrast of the particles, which indicate that the initial powders continue to exist in the form of small particles agglomerates. EDS mapping analyses presented in Fig. 10

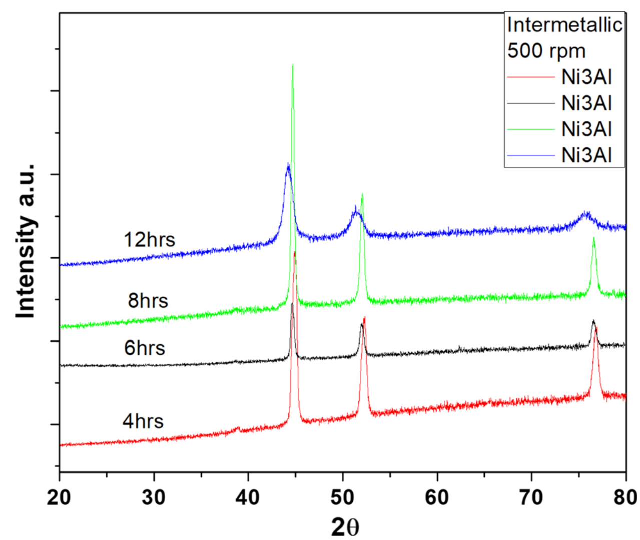

Fig. 8 X-ray diffraction patterns for the Ni-Al system mechanically alloyed at 500 rpm

show highly deformed aluminum particles embedded with noticeably smaller copper and nickel particles, clearly demonstrating the impact that both the size and high ductility of the aluminum phase has on the refinement process. These results indicate that under these conditions the predominant phenomenon during the milling process is particle fracture and consequently, that the energy of the system is not enough to achieve adequate atomic diffusion.

It is observed in the SEM images shown in Fig. 11 corresponding to samples obtained at 450 rpm that these are in accordance with the x-ray results regarding the formation of intermetallic particles with irregular shape after 24 h, which have an average size of 6 µm, It is necessary to highlight that in the images a greater homogenization can be observed than in the sample at 400 rpm because in this case, when increasing the energy of the system, there is a greater balance of cold and fracture welding processes, as well as atomic diffusion that gave rise to the formation of the Ni_3Al intermetallic phase. Consistently with the SEM images and x-ray diffraction,

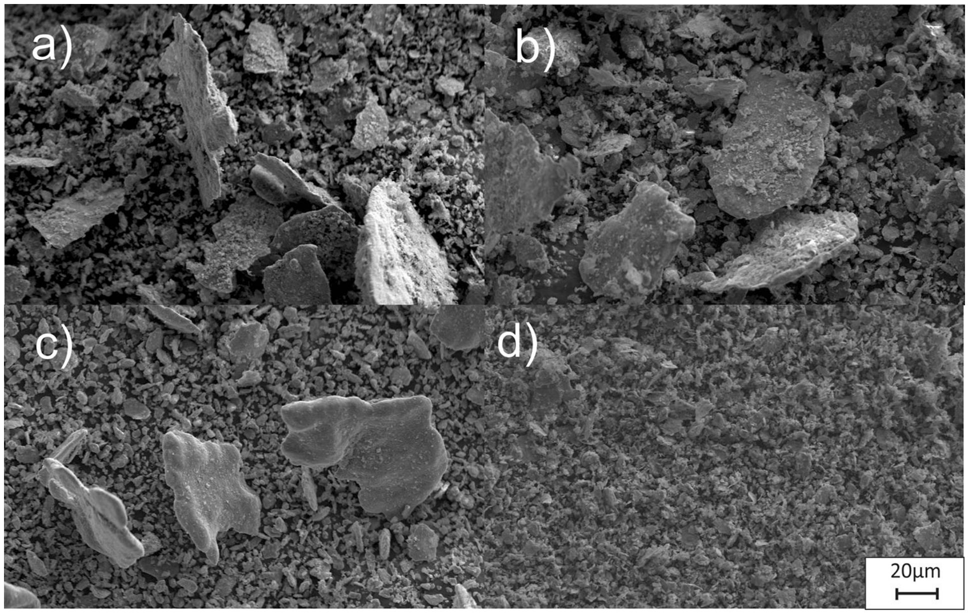

Fig. 9 SEM images of the Ni-Al-Cu system mechanically milled at 400 rpm for (a) 8 h, (b) 16 h, (c) 20 h and (d) 32 h

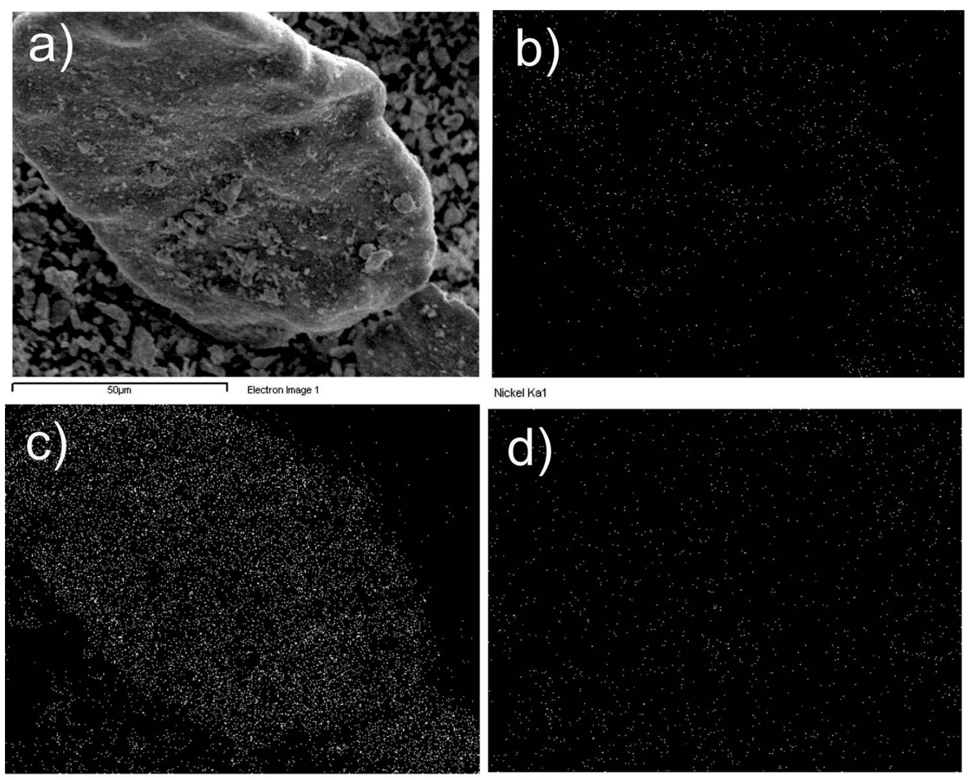

Fig. 10 SEM-EDS Ni-Al-Cu intermetallic particles obtained at 400 rpm for 20 h; (a) electron image, (b) Nickel, (c) Aluminum and (d) Copper

chemical EDS mapping analyses are presented in Fig. 12 show that there is a homogenous distribution of the elements in the particles, which indicates that there was a correct homogenization in the milling process.

One of the most interesting findings of this work consists in the considered reduction of the synthesis time for the samples. It is observed that under the conditions of 500 rpm and 12 h, the morphology of the particles is more homogeneous than those for the conditions of 400 and 450 rpm. For the milling process carried out at 500 rpm for 4 h, the initial powders were refined at an average particle size of 5 µm (Fig. 13a), meanwhile for the sample obtained at 400 rpm the necessary time to achieve the

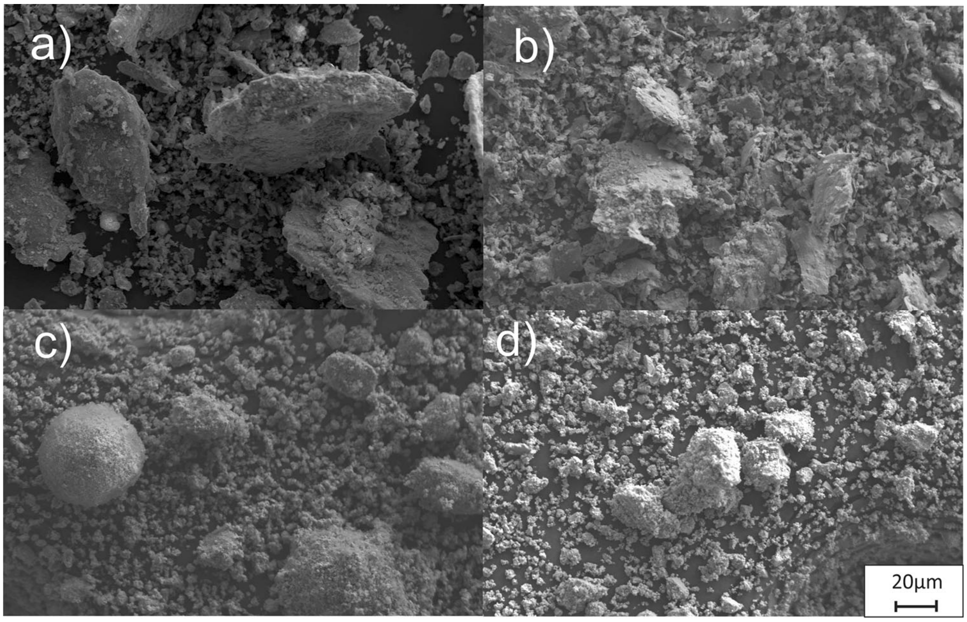

Fig. 11 Ni-Al-Cu intermetallic particles obtained at 450 rpm for (a) 8 h, (b) 16 h, (c) 24 h and (d) 30 h

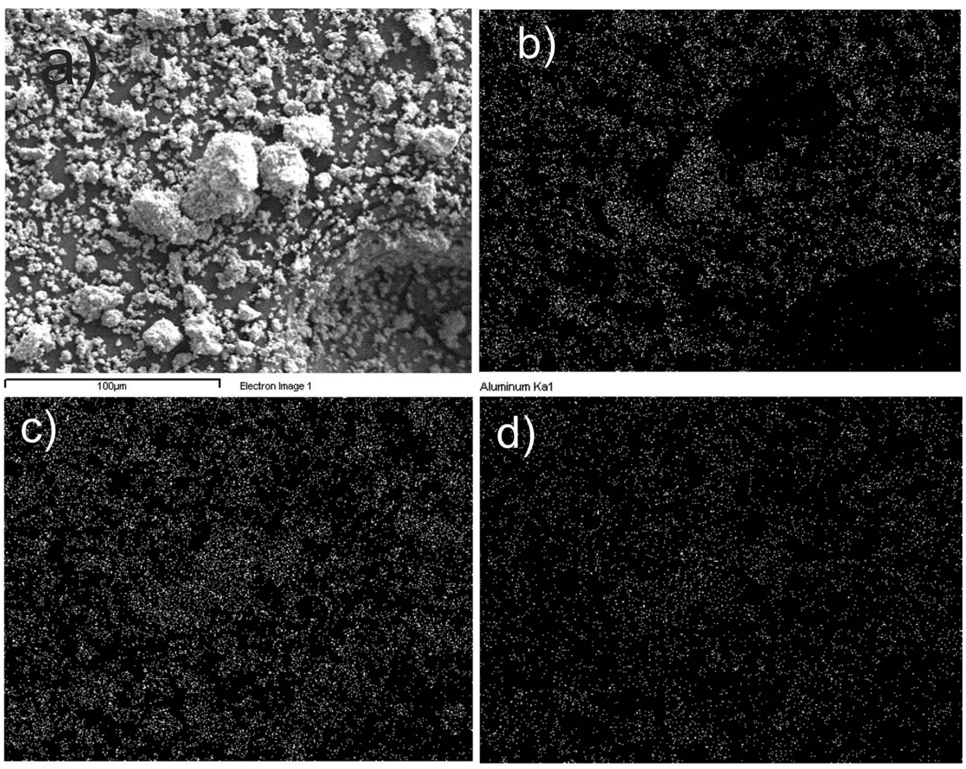

Fig. 12 SEM-EDS Ni-Al-Cu intermetallic particles obtained at 450 rpm for 30 h; (a) electron image, (b) Nickel, (c) Aluminum and (d) Copper

refinement was of 32 h (Fig. 9d); for the milling speed of 500 rpm, the formation of the Ni_3Al intermetallic phase occurred when the milling time was of 8 h (Fig. 13b); and for a milling time of 12 h, the morphology of the particles was semispherical. The SEM-EDS mapping results presented in Fig. 14 show that the intermetallic has a more homogeneous distribution of atoms in all particles.

4. Conclusions

In the synthesis of intermetallic $(Ni, Cu)_3Al$ it was observed that at 400 rpm it takes more than 32 hours of milling to form the intermetallic phase, while at 500 rpm the system only needs 8 hours, in addition, that the system does not present second phases after mechanical alloying. Observations carried out by SEM indicate that conditions of (a) 400 rpm the particles of the

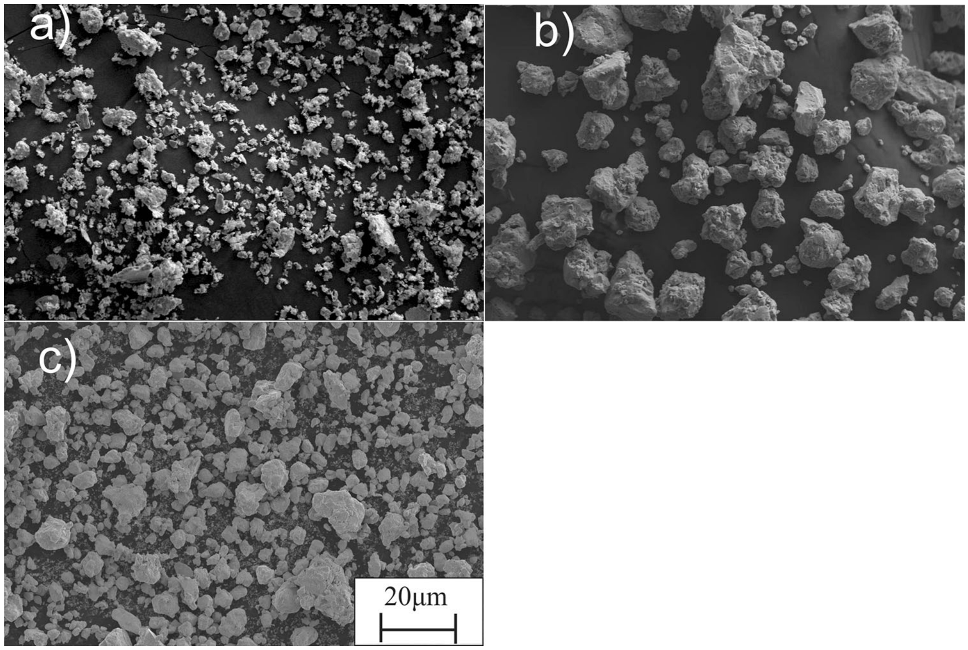

Fig. 13 Ni-Al-Cu intermetallic particles obtained at 500 rpm for (a) 4 h, (b) 8 h, (c) 12 h

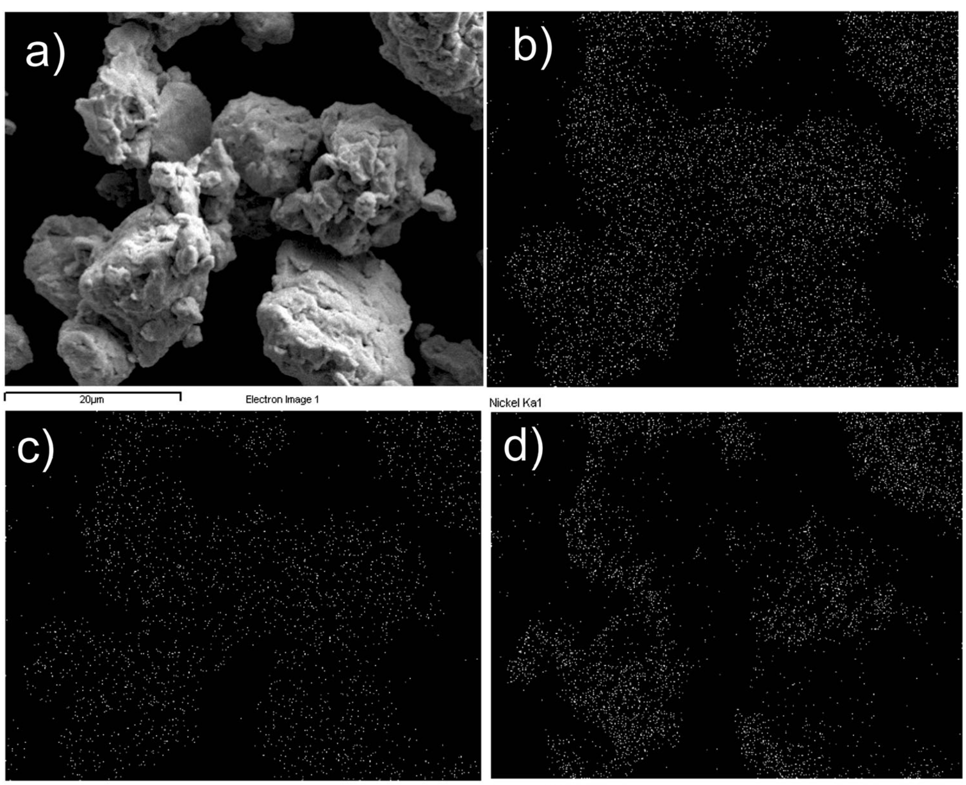

Fig. 14 SEM-EDS Ni-Al-Cu intermetallic particles obtained at 500 rpm for 8 h; (a) electron image, (b) Nickel, (c) Aluminum and (d) Copper

base materials can only be refined; (b) 450 rpm the intermetallic phase is formed, but having an irregular particle morphology, and (c) 500 rpm the intermetallic phase is formed with more homogeneous particles.

Therefore, the mechanical alloying technique is capable of synthesizing tailored intermetallic powders with good homogenization, providing more flexibility and control than that of conventional methods such as melting, nevertheless, it requires the correct processing parameters in order to allow atomic diffusion and subsequently phase changes take place. Very ductile materials such as Al seem to require higher amounts of energy when mechanically alloyed with very hard materials like Ni in order to find a balance between the diffusion and fracture events during the milling process.

Acknowledgements

This work was supported by PRODEP/SEP-MEXICO (Nos 511-6/2019.-15189).

References

1. N. Ivanova, The Electrochemistry of Intermetallic Compounds: A Mini-Review, *Electrochem. Commun.*, 2017, **80**, p 48–54
2. M.N. Samani, A. Shokuhfar, A.R. Kamali and M. Hadi, Production of A Nanocrystalline Ni_3Al-Based Alloy Using Mechanical Alloying, *J. Alloy. Compd.*, 2010, **500**, p 30–33
3. S.C. Hanyaloglu, B. Aksakal and I.J. McColm, Reactive Sintering of Electroless Nickel-Plated Aluminum Powders, *Mater. Charact.*, 2001, **47**, p 9–16
4. V.K. Portnoy, A.M. Blinov, I.A. Tomilin, V.N. Kuznetsov and T. Kulik, Formation of Nickel Aluminides by Mechanical Alloying and Thermodynamics of Interaction, *J. Alloy. Compd.*, 2002, **336**, p 196–2001
5. A. Mohammadnejad, A. Bahrami, M. Sajadi and M.Y. Mehr, Spark Plasma Sintering of Ni3Al-xB-1wt.% CNT (0.0 $< x <$ 1.5 at.%) Nanocomposite, *J. Alloy. Compd.*, 2019, **788**, p 461–467
6. M.E.N.G. Jie, J.I.A. Chengchang and H.E. Qing, Fabrication of Ni3Al by Hot Pressing from Element Powders, *Rare Met.*, 2007, **26**(3), p 222–225
7. Z.B. Jiao, J.H. Luan and C.T. Liu, Strategies for Improving Ductility of Ordered Intermetallics, *Progress Nat. Sci. Mater. Int.*, 2016, **26**(1), p 1–12
8. P. Mardiha, A. Bahrami, A. Mohammadnejad, Towards a High Strength Ductile Ni/Ni3Al/Ni Multilayer Composite using Spark Plasma Sintering. Sci. Sinter. 51, 4 (2019)
9. W. Zhao, Z. Sun and S. Gong, Synergistic Effect of Co-Alloying Elements on site Preferences and Elastic Properties of Ni3Al: A First-Principles Study, *Intermetallics*, 2015, **65**, p 75–80
10. D.E. Kim, S.L. Shang and Z.K. Liu, Effects of Alloying Elements on Elastic Properties of Ni3Al by First-Principles Calculations, *Intermetallics*, 2010, **18**, p 1163–1171
11. W. Gong, W. Zhao, N. Miao, J. Zhou, Z. Sun, S. Li and S. Gong, Strengthening Effects of Alloying Elements W and Re on Ni3Al: At First-Principles Study, *Comput. Mater. Sci.*, 2018, **144**, p 23–31
12. Y. Yu, J. Zhou, J. Chen, H. Zhou, C. Guo and B. Guo, Synthesis of Nanocrystalline Ni3Al by Mechanical Alloying and its Microstructural Characterization, *J. Alloy. Compd.*, 2010, **498**, p 107–112
13. K. Zhang, Z. Zhang, X. Lu, K. Li, Y. Du, J. Long, Y. Kong, Microstructure and composition of the grain/binder interface in WC–Ni3Al composites. Int. J. Refract. Metals Hard Mater. 44, 88–93 (2014)
14. J. Colín, S. Serna, B. Campillo, R.A. Rodríguez and J. Juárez-Islas, Effect of Cu Additions Over the Lattice Parameter and Hardness of the NiAl Intermetallic COMPOUND, *J. Alloy. Compd.*, 2010, **489**, p 26–29
15. J. Colín, S. Serna, B. Campillo, O. Flores and J. Juárez-Islas, Microstructural and Lattice Parameter Study of As-Cast and Rapidly Solidified NiAl Intermetallic Alloys with Cu Additions, *Intermetallics*, 2008, **16**, p 847–853
16. S. Deng, J. Li, R. Li, H. Zhao, T. Yuan, L. Li and Y. Zhang, The Effect of Particle Size on the Densification Kinetics of Tungsten Powder During Spark Plasma Sintering, *Int. J. Refract Metal Hard Mater.*, 2020, **93**, p 105358
17. L. Lü and M.O. Lai, *Mechanical Alloying*, Springer, New York, 2013
18. S. Ameri, Z. Sadeghian and I. Kazeminezhad, Effect of CNT Addition Approach on the Microstructure and Properties of NiAl-CNT Nanocomposites Produced by Mechanical Alloying and Spark Plasma Sintering, *Intermetallics*, 2016, **76**, p 41–48
19. M.B. Vishlaghi and A. Ataie, Investigation on Solid Solubility and Physical Properties of Cu–Fe/CNT Nano-Composite Prepared via Mechanical Alloying Route, *Powder Technol.*, 2014, **268**, p 102–109
20. A. Mohammadnejad, A. Bahrami, M. Sajadi, P. Karimi, H.R. Fozveh and M.Y. Mehr, Microstructure and Mechanical Properties of Spark Plasma Sintered Nanocrystalline Ni_3Al-xB (0.0$< x <$ 1.5 at.%) alloy, *Mater. Today Commun.*, 2018, **17**, p 161–168
21. C. Zhang, K. Feng, Z. Li, F. Lu, J. Huang and Y. Wu, Microstructure and Mechanical Properties of Sputter Deposited Ni/Ni3Al Multilayer Films at Elevated Temperature, *Appl. Surf. Sci.*, 2016, **378**, p 408–417
22. C.G. Ferguson, K.A. Christofidou, E.M. Hildyard, A.S. Wilson, N.G. Jones and H.J. Stone, On the Continuous and Discontinuous Precipitation of the L12 Phase in Cu-Ni-Al Alloys, *Materialia*, 2020, **13**, p 100855